

INPUT MATERIAL DATA FOR ADVANCE COMPUTATIONAL MODELS FOR FORMING STAINLESS MATERIAL

SOBOTKA Jiří, SOLFRONK Pavel, KOLNEROVÁ Michaela, ZUZÁNEK Lukáš

TUL - Technical University of Liberec, Liberec, Czech Republic, EU

jiri.sobotka@tul.cz, pavel.solfronk@tul.cz, michaela.kolnerova@tul.cz, lukas.zuzanek@tul.cz

Abstract

During the last years there is a strong tendency of automotive industry to achieve suitable compromise between effort to lower environmental load at car operation by lowering its weight (thus to lower thickness of used parts) and on the other hand there is tendency to still increase the safety of passengers by utilization ultra-high strength materials. That is why these days are more and more important strength materials and alloys based e.g. on aluminium or magnesium. However industrial processing of these materials reveals quite a lot of problems. Thus these days there is a great demand for high-quality computational models within the numerical simulations for processing these materials because quite great portion of producing problems can be eliminated by pre-producing phase using numerical simulations (FEA). For precious numerical simulations computation is, beside geometry of part and tool, very important selection and accuracy of material input data subsequently regarding also selection of own computational model. During the last years there were developed a lot of computational models which within the metal forming regard yield criterions. One of these yield criterions is also anisotropic computational model named as Vegter model. The purpose of this paper is not only to describe such computational model but mainly to show procedure of measurement the most important input material data for stainless material to be computed by Vegter model. Such measurement is not only about static tensile test but there is used also the hydraulic bulge test to determine so-called bi-axial point in Vegter model.

Keywords: Yield Criterion, Computational Model, Numerical Simulation, Hydraulic Bulge Test, Stainless Material

1. INTRODUCTION

Numerical simulations and computational models represent one of crucial factors during pre-producing phase for any product. However their reliability (or more precisely reliability of their results and matching with reality) is greatly influence by used input data. Moreover there is not only problem with reliability of these data but also with the wide range of different materials when some of them are quite newly used or have been just developed (e.g. some ultra high-strength steels, aluminium alloys, magnesium alloys and so on). In this paper was tested stainless steel with the purpose to describe whole methodology how to find out such relevant input data to be used in advance computational models (e.g. in Vegter yield criterion). Three basic pillars of numerical simulations can be summarized as following: the static tensile test (stress-strain curve), normal anisotropy coefficients and forming limit diagrams. However for the modern computational models (or more precisely for different yield criterions) much more other results are necessary. Among them can be found mainly position of so-called bi-axial point which can be determinate e.g. via the hydraulic bulge test. Sometimes can be also required positions of plane-strain points which makes own testing much more time consuming. That is why in this paper was for experiments used firstly static tensile test and then hydraulic bulge test and the main purpose was to find out all important constants for their future utilization in advance computational models. In both cases there was used fitting of stress-strain curve by Swift's equation (1).

2. METHODOLOGICAL BASE AND EXPERIMENTAL PART

The most important part of this papers deals with the own measuring, computing and fitting all important constants for their future utilization in the advance computational models of sheet forming (mainly Vegter yield criterion). That is why first part of testing stainless steel was about the static tensile test and its approximation by Swift's equation and the second part dealt with the hydraulic bulge test.

2.1. Static tensile test

As was already mentioned, first part from the experiment was about the static tensile test. This test was carried out under common testing conditions and basic results are summarized in **Table 1**. As a major output from this measurement there was stress-strain curve and mainly its approximation acc. to Swift - see **Fig. 1**.

Table 1 Mechanical properties of the tested material (stainless steel - DIN 1.4301)

| Rolling direction (°) | Yield strength R _{p0.2} (MPa) | Ultimate strength R _m (MPa) | Uniform ductility A _g (%) | Total ductility A _{80mm} (%) | Strength coefficient C (MPa) | Strain hardening exponent n (1) | Plastic strain equivalent φ ₀ (1) |
|-----------------------|--|--|--------------------------------------|---------------------------------------|------------------------------|---------------------------------|--|
| 0° | 288.9 | 647.1 | 47.85 | 53.58 | 1464.2 | 0.4980 | 0.0400 |
| 45° | 277.2 | 612.4 | 54.77 | 61.50 | 1474.7 | 0.4983 | 0.0406 |
| 90° | 283.7 | 624.7 | 55.14 | 60.8 | 1378.4 | 0.5154 | 0.0478 |

For the subsequent utilization of stress-strain curve from static tensile (thus at uni-axial tensile stress state) there was necessary to compute three constants from so-called Swift's equation which is modification of the Hollomon equation - see equation (1) and **Fig. 1** (meaning of these constants is evident from **Table 1**). [1]

$$\sigma_{TR} = C \cdot (\phi_{TR} + \phi_0)^n \tag{1}$$

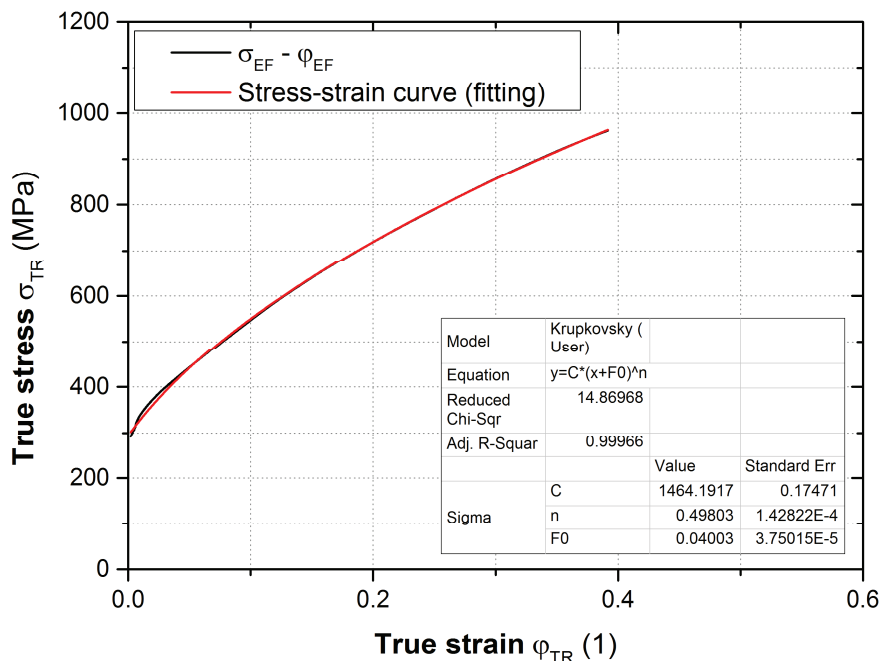


Fig. 1 Approximation of stress-strain curve from static tensile test - stainless steel (rolling direction 0°)

2.2. Hydraulic bulge test

The hydraulic bulge test represented the second major part of the experiment. For this test is very important fact that there is bi-axial stress state cause it is very important “point” for the future utilization for different yield criterions. Due to the different stress state in comparison to the static tensile test, for its stress-strain curve it is necessary to compute so-called the effective stress σ_{EF} (MPa) and effective strain φ_{EF} (1). Computation of all important values is written by means of equation (2), (3) and (4). [2]

$$\sigma_{EF} = \frac{pR}{2t} \quad (2)$$

$$\varphi_{EF} = \frac{2\sqrt{3}}{3} \sqrt{\varphi_1^2 + \varphi_1\varphi_2 + \varphi_2^2} \quad (3)$$

$$\varphi_{EF} = \frac{2\sqrt{3}}{3} \sqrt{\varphi_1^2 + \varphi_1\varphi_2 + \varphi_2^2} \quad (4)$$

$$t = t_0 \cdot e^{-\varphi_3}$$

where:

| | | | | | |
|-------------------|--------------------|--------|----------|--------------------------------|--------|
| σ_{EF} | - effective stress | (MPa); | p | - pressure | (MPa); |
| φ_{EF} | - effective strain | (1); | R | - radius of curvature | (mm); |
| $\varphi_{1,2,3}$ | - true strains | (1); | t, t_0 | - actual and initial thickness | (mm). |

For the own measurement of the hydraulic bulge test there was used contact-less optical system ARAMIS. The principle of such measurement is shown in **Fig. 2**. Measured material is placed between upper and lower blank-holders and two scanning cameras are added right before the tested material (stainless steel in this case). That transparent glass needs to be clear after every test because just after fracture of material (in this case it was under pressure 22 MPa), hydraulic oil is jetting up towards cameras. Because it is optical system, there is very important to properly adjust cameras (calibration, shutter time, focusing, distances, angles and so on) and provide proper lighting for the whole scanning area.

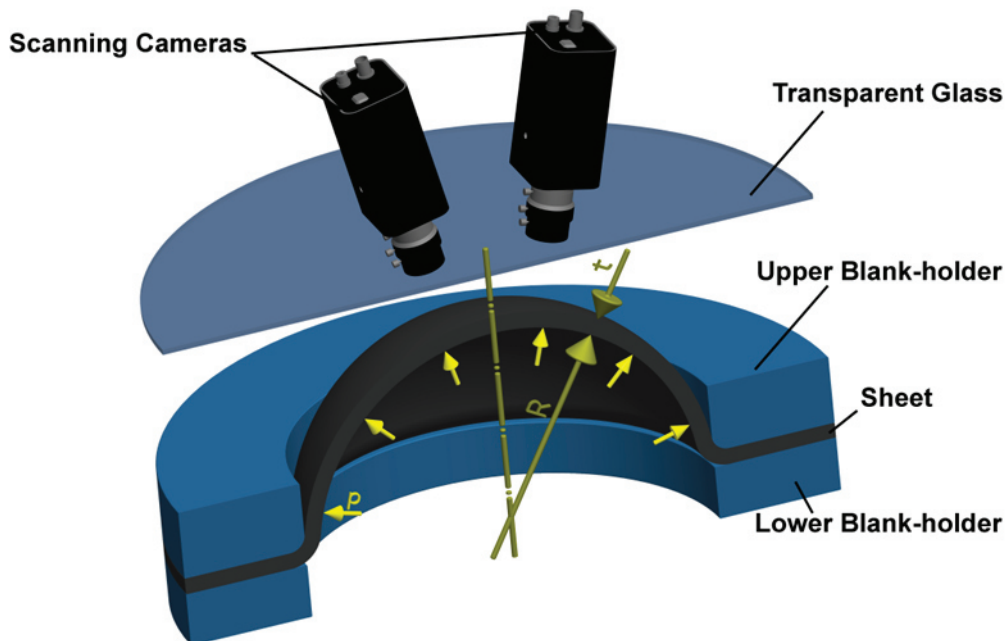


Fig. 2 Principle of the hydraulic bulge test with contact-less optical system ARAMIS

In **Fig. 3** are shown images scanned just from the left camera during the whole hydraulic bulge test - on the left is image and strain distribution for stage 0 (so blue color for strain distribution $\varphi_1 = 0$) and on the right is shown the same but in this case for stage 316 (pressure $p = 18$ MPa). Small "holes" are due to insufficient adjustment of cameras or bad light conditions.

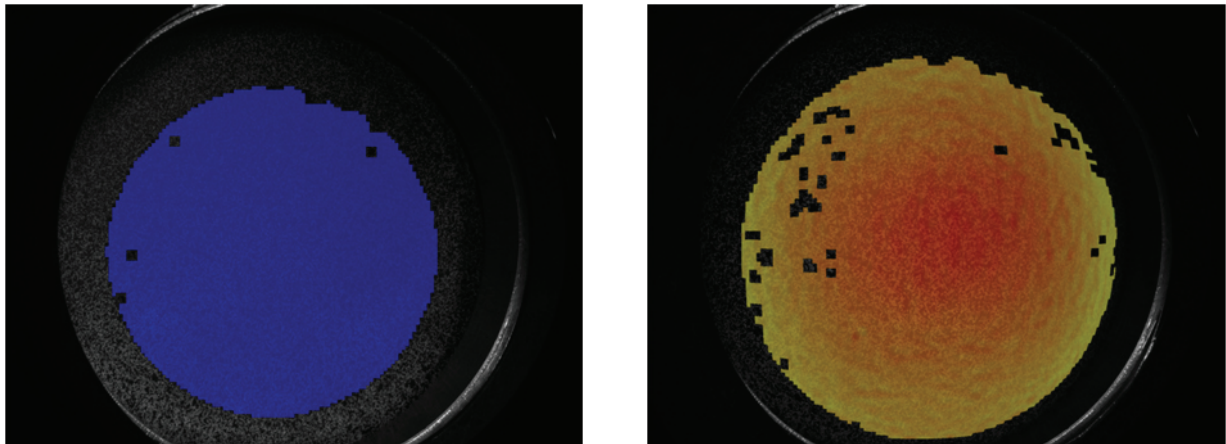


Fig. 3 Distribution of major strain φ_1 [1] - stage 0 (left) and stage 316 (right)

As the whole evolution of the hydraulic bulge test was scanned by contact-less optical system ARAMIS, subsequently it was possible to compute distribution of both major strain φ_1 (1) and minor strain φ_2 (1) within the required area (top of the sphere). Due to that was also possible to compute strain in the thickness direction φ_3 (1) which is important to know to be able to compute actual thickness - see equation (4). Finally by fitting best-fit sphere over computed part of sphere (see **Fig. 4**) it was possible to find out required radius of curvature R [mm]. In **Fig. 4** is shown such best-fit sphere again for stage 316 (pressure $p = 18$ MPa). After that was possible with equations (2), (3) and (4) to compute required effective stress σ_{EF} (MPa) and effective strain φ_{EF} (1) and to plot stress-strain curve for bi-axial state of stress (hydraulic bulge test) - see **Fig. 5**.

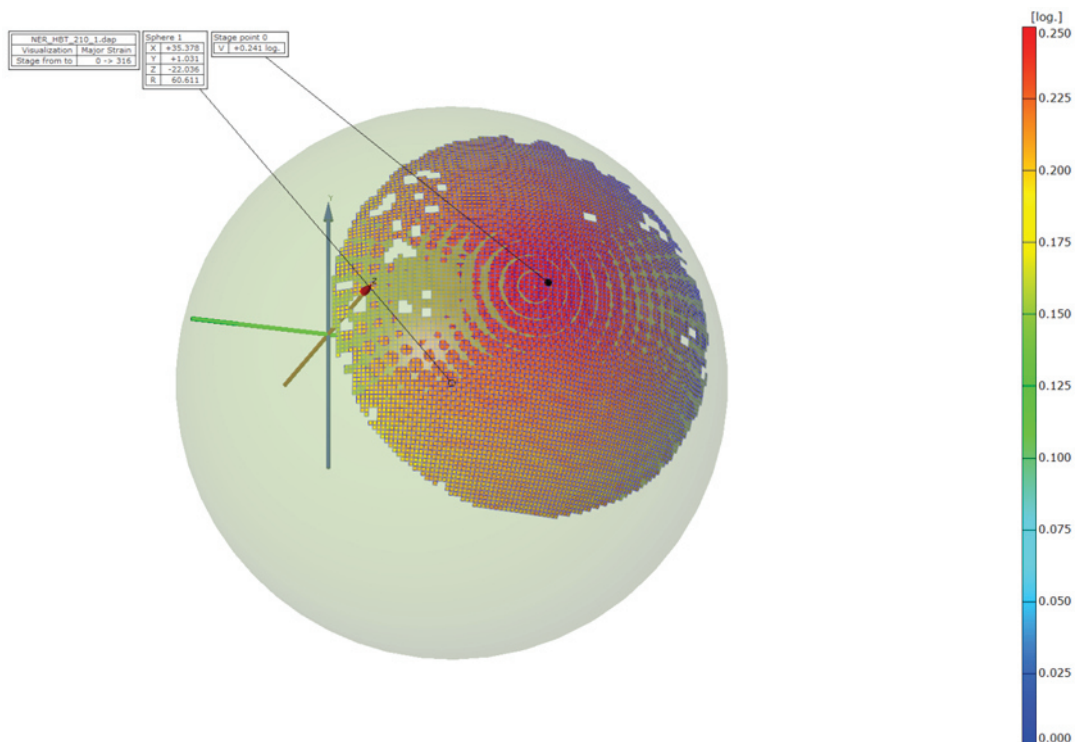


Fig. 4 Application of best-fit sphere (stage 316; pressure $p = 18$ MPa)

In **Table 2** are summarized all important values to plot required stress-strain curve of stainless steel. Because of space there is written every second used pressure (in fact it was from 1 up to 18 MPa á 1 MPa).

Table 2 Results of the hydraulic bulge test (stainless steel; initial thickness $t_0 = 0.805$ mm)

| Stage | Pressure p (MPa) | Radius of curvature R (mm) | Actual thickness t (mm) | Effective stress σ_{EF} (MPa) | Effective strain φ_{EF} (1) |
|-------|--------------------|------------------------------|---------------------------|--------------------------------------|-------------------------------------|
| 26 | 2 | 261.964 | 0.786 | 336.906 | 0.022 |
| 62 | 4 | 155.850 | 0.757 | 411.961 | 0.059 |
| 98 | 6 | 120.380 | 0.727 | 497.281 | 0.099 |
| 134 | 8 | 101.062 | 0.698 | 579.228 | 0.140 |
| 170 | 10 | 88.348 | 0.668 | 661.582 | 0.183 |
| 206 | 12 | 79.171 | 0.636 | 745.930 | 0.231 |
| 243 | 14 | 72.094 | 0.602 | 838.297 | 0.287 |
| 279 | 16 | 66.299 | 0.562 | 943.207 | 0.354 |
| 316 | 18 | 60.611 | 0.504 | 1082.520 | 0.462 |

From these values was subsequently created the scatter plot - see **Fig. 5**. It is not possible to use continuous increasing of pressure due to time delay in sensor and hoses. After that was also used (as in the case of the static tensile test) the power-law equation acc. to Swift and via fitting (nonlinear curve fit) was computed stress-strain curve and all important constants (C , n , φ_0). Values of these constants for the hydraulic bulge test were as following: $C = 1675.6$ MPa, $n = 0.6617$ and $\varphi_0 = 0.0622$. Such values are truly very important to compute so-called bi-axial point in advance computational models in numerical simulations (e.g. for Vegter yield criterion). Beside values of uni-axial tensile (eventually compression) point and normal anisotropy coefficients are these values the crucial for proper computation of required yield criterions.

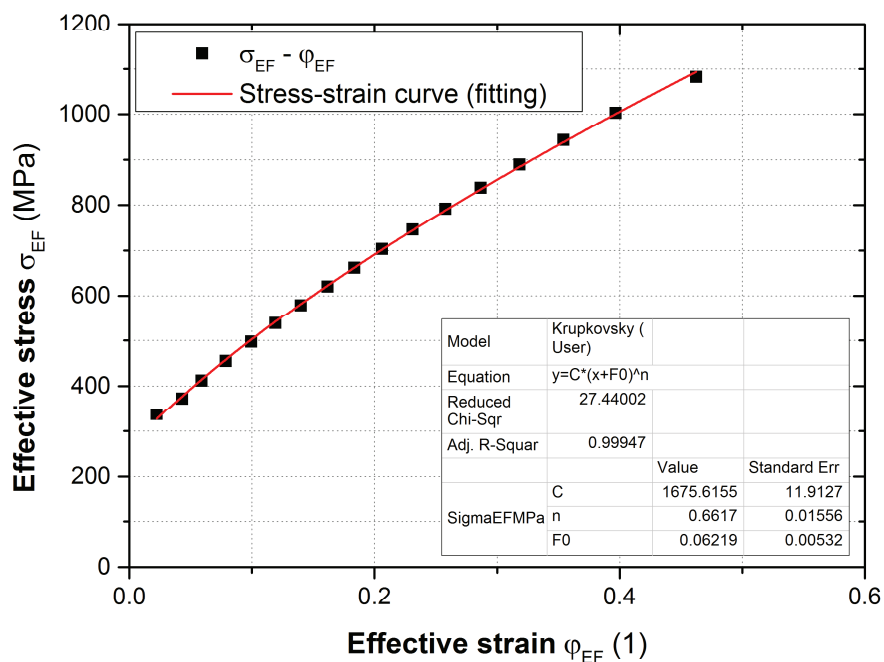


Fig. 5 Approximation of stress-strain curve from the hydraulic bulge test (stainless steel - DIN 1.4301)

3. CONCLUSION

This paper deals with the description how to measure and evaluate important input material data for advance computational models for forming stainless material. That is why this paper was divided into two major experimental parts - the static tensile test and the hydraulic bulge test. In **Fig. 6** is shown their mutual comparison via stress-strain curves. As a tested was chosen stainless steel (DIN 1.4301) because it very properly represents one of the basic material types which are still more and more used in the automotive industry these days - (ultra) high-strength steel to improve safety of passengers. From this **Fig. 6** is also evident influence arising from the different stress states between the static tensile test and the hydraulic bulge test - thus the uni-axial tensile stress state and the equi bi-axial stress state. However for both these parts there was an effort how to evaluate all important constants for their future utilization and processing in the advance computational models as can be e.g. Vegter yield criterion which is still more and more used these days mainly in the automotive industry. Thus from both experimental tests were computed (via approximation of stress-strain curves) especially following constants: strength coefficients C (MPa), strain hardening exponents n (1) and plastic strain equivalent φ_0 (1) for stainless material. Together with normal anisotropy coefficients and forming limit diagrams represent these constants basic pillars to be used in modern numerical simulations and their computational models. It is evident that their measurement is quite time consuming but it is very important for the accuracy of numerical simulations so it can save a lot of energy and money during pre-producing phase. Such results are obvious when utilization different computational models and their matching with reality (e.g. real car-body panels) [3].

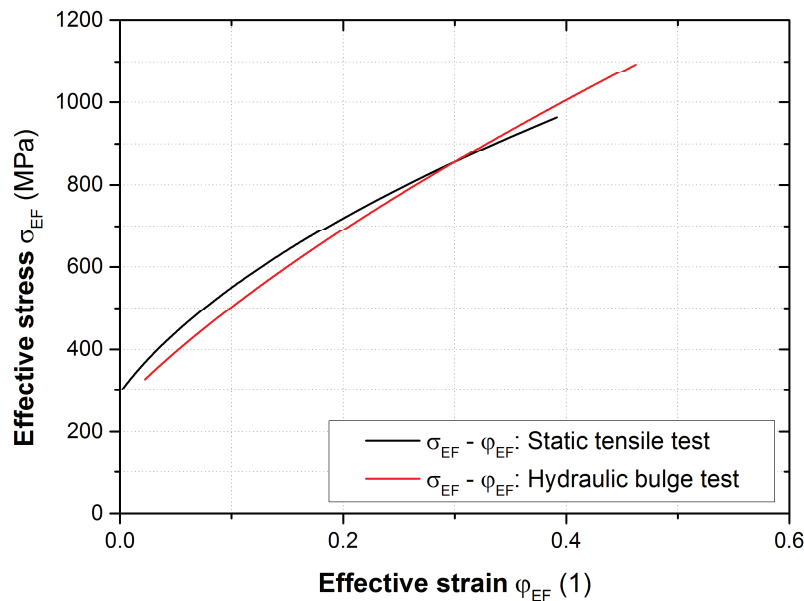


Fig. 6 Stress-strain curves comparison of static tensile test and hydraulic bulge test

REFERENCES

- [1] ASM HANDBOOK. Volume 14B - Metalworking: Sheet Forming. 2nd ed. Materials Park: ASM International, 2006.
- [2] HOSFORD, W.F., CADDEL, R. Metal Forming (Mechanics and Metallurgy). 3rd ed. New York: Cambridge University Press, 2007.
- [3] DAVIES, G. Materials for Automobile Bodies. Oxford: Butterworth-Heinemann, 2003.